Uncertainty, topography, and work function

Ivor Brodie*
Physical Electronics Laboratory, SRI International, Menlo Park, California 94025
(Received 9 September 1994; revised manuscript received 9 January 1995)

A simple procedure has been found that enables the zero-temperature, zero-field work function for elemental crystal surfaces to be estimated within a few tenths of an eV. It uses the local-density-approximation value for the Fermi energy to obtain the Heisenberg uncertainty distance, equates this distance to the distance from the surface at which the image force begins to act, and further assumes that the image force acts as if it were done to an isolated conducting sphere of the same radius as that of the atoms of which the surface is composed. The importance of this result is that it gives a clear physical picture of the emission process that takes into account the microscopic surface structure, and lends credence to the concept of continuous decoherence from quantum to classical states. Variation of work function between crystal faces is plausibly shown to be mainly due to variation with direction of the effective mass of an electron with the Fermi energy inside the crystal. Work functions of optimum electropositive monolayer adsorbates on refractory metal substrates calculated by this method also agree closely with experiment, indicating that the electrons are emitted from exposed substrate atoms. A model for the topological structure of a crystal surface on an atomic scale is proposed for which classical methods indicate that the field at the tips of the atoms is typically 2.5 times that estimated on the basis that the surface is a smooth plane. The consequential effect on thermionic and field emission is discussed. Order-of-magnitude estimates of the variation of the work function with temperature and stress are also made.

I. INTRODUCTION

With the advent of modern high-speed computers and the development of sophisticated algorithms it has become practical to compute from first principles, without adjustable parameters and using only the Schrödinger equation, many of the physical properties of crystalline solids,[1] using a local-density approximation (LDA) to account for electron-electron and electron-core interactions. In particular, the density of states in the conduction band and the Fermi energy at 0 K can be precisely calculated, and the zero-temperature, zero-field work function for the various crystal faces of metals can be estimated within a few tenths of an eV.[1,2] By making other approximations the speed of computation may be increased, and work functions for various crystal faces of 40 elemental metals have been calculated[3] with results that agree with experiment within a few tenths of an eV.[4]

The importance of the present work lies in its ability to give a clear physical picture of the electron emission process from a metal surface that takes into account the surface structure at an atomic level and, with its ability to predict average work functions within a few tenths of an eV, lends credence to the concept of continuous decoherence from quantum to classical states.[5–7] It is possible not only to estimate the work function of a surface very simply but also to gain an insight into the effect of surface structure at an atomic level on the electron emission process.

The results obtained from scanning tunneling microscopy[8] show conclusively that for metallic crystals a surface can be identified that behaves as a classical metal electrode to subangstrom precision. This surface can be represented as an array of atomic-sized spheroids, and the tips of the spheroids may reasonably be assumed to have a radius close to that of an isolated atom of the species involved.

The work function may be defined as the smallest amount of energy that must be given to an electron with the Fermi energy inside a solid that is normally approaching an interface between the solid and vacuum to enable it to be transported to a field-free region external to the surface, when the solid is at a temperature of 0 K and there is zero applied electric field at the surface. It is perhaps most accurately measured by the appearance photon energy for photoelectric emission from a surface.[4]

The force of an electron external to the metal surface, without applied fields, is due to the charge induced on the metal surface by the unscreened Coulomb interaction of the electron on the surface. Classically, this is obtained by assuming a "virtual" image charge inside the conductor. There is a region bounded by a surface spaced d from the classical metal surface that an electron inside the metal can transverse by converting its kinetic energy to potential energy without doing any work. At d the kinetic energy of the electron is zero and it is assumed that at this point the classical image force begins to act. The work function is then the energy that has to be given to an electron to take it from d where it has zero kinetic energy to a field-free region far enough away from the metal surface for the image force to be zero. The use of such a surface where the image force becomes effective was traditionally used in the early theories[9] and has been theoretically justified by using a first-principles evaluation of the exchange-correlation potential for the electron-gas–vacuum interface.[10,11]

Inside the metal, quantum theory is required to determine the highest kinetic energy an electron may have at 0 K as it approaches the classical metal surface (namely, the Fermi energy ε_F). Beyond d, classical mechanics is adequate to determine the work function. Between the classical metal surface and the d surface, the momentum changes from $(2\varepsilon_F/m^*)^{1/2}$ to zero, where m^* is the effective mass of the electron inside the metal as it approaches the surface. We identify the distance d with the Heisenberg uncertainty distance associated with this change in momentum, as appears to be required by continuous decoherence from quantum to classical states. In appropriate cases the use of the uncertainty relation to bypass equivalent but more complex methods of solving wave equations is well known. For example, it can be used to directly obtain exact values for the ground-state energy and radius of the hydrogen atom.[12] When we consider the difficulties of measuring work functions to better than 0.1 eV, and the lack of data on effective masses, the remarkable agreement with experimental values, as given below, support the validity of this model, and offers a proof of the validity of the principle of continuous decoherence (see Sec. VII).

II. ESTIMATING THE WORK FUNCTION

To estimate the effect of a surface consisting of an array of spheroids on the image force we consider first the image force on an electron charge $-e$ distant $(R+u)$ from the center of a conducting sphere of radius R. The image charge inside the sphere has a value[13]

$$+q=eR/(R+u) \tag{1}$$

and is located on a line joining the center of the sphere with the electron at a distance from the center given by

$$z=R^2/(R+u)\ . \tag{2}$$

Thus the distance of the electron from its image is $[(R+u)-z]$ and the attractive force between them is

$$F_1=qe/4\pi\xi_0[(R+u)-z]^2\ , \tag{3}$$

where ξ_0 is the permittivity of free space. Using Eqs. (1) and (2) in (3) gives

$$F_1=[e^2/4\pi\xi_0]\{R(R+u)/[(R+u)^2-R^2]^2\}\ . \tag{4}$$

If a potential is applied to a distant concentric spherical anode such that it produces an electric field E_0 at the surface of the cathode, then the magnitude of the field at a point distant $(R+u)$ from the center is given by

$$E(u)=E_0R^2/(R+u)^2 \tag{5}$$

and the force on an electron due to this field acts to pull the electron away from the surface and is given by

$$F_2=eE_0R^2/(R+u)^2\ . \tag{6}$$

Thus the net force on the electron is

$$F=F_2-F_1=[eE_0R^2/(R+u)^2]-[e^2/4\pi\xi_0]\times\{R(R+u)/[(R+u)^2-R^2]^2\}\ . \tag{7}$$

The zero-field work function (in eV) is given by

$$e\phi=\int_d^\infty F_1\,du \tag{8a}$$

or

$$\phi=(e/8\pi\xi_0)\{R/[(R+d)^2-R^2]\}=7.19\times10^{-10}\{R/[(R+d)^2-R^2]\}\ . \tag{8b}$$

For the case of a planar surface $(R\to\infty)$

$$\phi=e/16\pi\xi_0 d \tag{9a}$$

or

$$\phi(\infty,d)=3.595/d \tag{9b}$$

for d in angstroms, the same value obtained when using the plane image force,[9] as expected. Note also (for R and d in angstroms) that

$$\phi(R,d)=\phi(\infty,d)/(1+d/2R)=3.595/d(1+d/2R)\ \text{eV} \tag{10}$$

and the difference between the plane and spherical work functions is

$$\delta\phi=\phi(\infty,d)-\phi(R,d)=3.595/(2R+d)\ \text{eV}\ . \tag{11}$$

Figure 1 shows ϕ as a function of d (in angstroms) with R as a parameter. The range of ϕ covered (0.5–8 eV) is the range of the work function for most real materials. Note the relatively small difference in the predicted values of ϕ for given d over a range of R from infinity to 1.25 Å.

There is also a distance u_0 at which the two forces on the electron are equal, given by the solution to Eq. (7) with $F=0$. The energy required to be given to an electron to escape is now

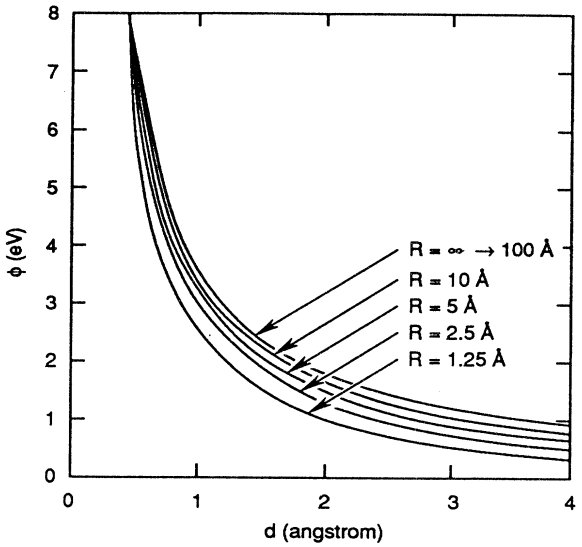

FIG. 1. Work function (ϕ) as a function of the distance d from the surface that an electron from the interior of a conductor of radius R reaches before experiencing its "image" force.

$$\phi' e = \int_0^{u_0} Ee\, du + \int_d^{u_0} [e^2/4\pi\xi_0]\{R(R+u)/[(R+u)^2-R^2]^2\}du \ . \quad (12)$$

Thus the Schottky lowering the work function due to the electric field[9] is given by

$$\Delta\varphi = \varphi - \varphi' = \int_{u_0}^{\infty} [e/4\pi\xi_0]\{R(R+u)/[(R+u)^2-R^2]^2\}du - \int_0^{u_0} E_0 R^2/(R+u)^2 du \ .$$

That is,

$$\Delta\phi = [e/4\pi\xi_0]\{R/[(R+u_0)^2-R^2]\} - E_0 R^2[1/R - 1/(R+u_0)] \ . \quad (13)$$

As R tends to infinity, the first term tends to the conventional Schottky relation for the lowering of the work function,

$$\Delta\phi = (eE_0/4\pi\varepsilon_0)^{1/2} = 3.792\times 10^{-5} E_0^{1/2} \quad (14)$$

for E_0 in V/m and the second term tends to zero, as expected.

If the energy of an electron inside the metal is measured from the bottom of the conduction band it represents essentially the kinetic energy of the electron. As an electron attempts to leave the surface, its kinetic energy ε in the escape direction is transferred to potential energy and there is a distance δx at which its kinetic energy is zero. Classically, it cannot move beyond this point. The change in momentum over this distance is given by

$$\Delta p = (2m^*\varepsilon)^{1/2} \ , \quad (15)$$

where m^* is the effective mass of the electron inside the metal.

According to the Heisenberg principle, the smallest uncertainty in the position of the electron when its momentum changes by Δp is given by

$$\Delta p\, \delta x = h/2\pi \ . \quad (16)$$

Thus

$$\delta x = h/2\pi(2m^*\varepsilon)^{1/2} \ . \quad (17)$$

For an electron at the Fermi energy $\varepsilon = \varepsilon_F$ the value of δx at 0 K is given by

$$\delta x = 1.953/\varepsilon_F^{1/2}(m^*/m)^{1/2} \ \text{Å} \ , \quad (18)$$

where m is the normal electron mass as measured in vacuum at low energies, and ε_F is measured in eV from the bottom of the conduction band. Since m^* varies with direction of motion of an electron relative to the lattice, the momentum of an electron associated with the Fermi energy will vary with direction, and the work function may be expected to vary with the crystal face from which an electron emerges. Identifying δx of Eq. (18) with d of Eq. (10), we obtain

$$\phi(R,d) = 1.841\varepsilon_F^{1/2}(m^*/m)^{1/2} \times [1 + 1.953/2R\varepsilon_F^{1/2}(m^*/m)^{1/2}]^{-1} \ . \quad (19)$$

Of the three quantities required to evaluate this equation for specific metals, the atomic radii R are well known[14] and the Fermi energy ε_F can be computed to a precision of less than 0.1 eV using the LDA,[1] but the effective masses m^* at the Fermi energy vary with direction of motion inside the crystal and procedures for obtaining them using the LDA have not yet been developed. In metals the effective mass of the electrons does not differ substantially from the rest mass, but the change is sufficient to cause differences in work function between different crystal faces of the same metal. Thus setting $m^*/m = 1$ will predict an average value of the work function that may be compared with the preferred experimental values obtained from randomly oriented polycrystalline surfaces[4] and from different crystal planes of the same metal crystal.

Table I compares work functions of some elemental metals from different parts of the periodic table estimated using the above model with experimental values for polycrystalline surfaces[4] and values obtained from the more conventional approach.[2,3] The values of the Fermi energy were computed for the author by Paxton and van Schilfgaarde[15] using programs based on the LDA.

It will be seen from Table I that the present approach predicts work functions within a few tenths of an eV of the measured work function for polycrystalline surfaces. The closest agreement is for Cu, Ag, and Au. The poorest is for Ti, which is 0.6 eV lower than the measured value. Next are W and Mo, which are 0.4 eV lower, and the remainder are less than 0.3 eV lower. These results compare well within the differences between predicted and measured work functions for specific crystal faces by the more comprehensive methods,[2,3] which as is shown in Table I can be as large as 0.7 eV. The present model could be used to predict values of work function for specific crystal faces if the corresponding m^*'s were known. However, if the validity of the present model is accepted, Eq. (19) can be used to estimate the effective mass of the electron in a given direction from measured values of the work function for specific crystal faces. This has been done for W using the measured values given in Table I, the results being given in Table II. The values of m^*/m so obtained are well within the range of what might be expected.

The important conclusion to be drawn from this discussion is that the zero-temperature, zero-field work function for elemental metal crystal surfaces can be estimated within a few tenths of an eV by using the LDA value of the Fermi energy to obtain the Heisenberg uncertainty distance, equating this distance to the distance from the surface at which the image force begins to act, and assuming the image force acts as if it were generated by an isolated sphere of the radius of the atoms of which the surface is composed. The latter point is important in that it argues that a large fraction of the electrons must be emitted from sites near the tips of the atoms where the image force will be close to that of isolated atoms. This point is discussed in more detail in Sec. IV.

TABLE I. Comparison between theoretical and experimental values for the zero-temperature, zero-field work function.

Parameter/element	Mo	W	Cs	Ba	Ti	Cu	Ag	Au
$2R$ (Å)[a]	2.80	2.82	5.40	4.48	2.93	2.551	2.883	2.878
ε_F (eV) computed[b]	8.01	10.46	1.76	2.85	6.50	9.75	8.21	10.44
$\delta x = d$ (Å) [Eq. (18)]	0.69	0.605	1.47	1.16	0.767	0.626	0.682	0.605
			ϕ (eV) calculated from Eq. (19)					
	4.18	4.90	1.92	2.47	3.72	4.62	4.26	4.91
			ϕ (eV) preferred experimental values[c] for polycrystalline surfaces					
	4.6	4.55	2.14	2.7	4.33	4.65	4.26	5.1
			ϕ (eV) preferred experimental values[c] for oriented crystal surfaces					
fcc(111)	4.55	4.47				4.98	4.71	5.31
fcc(100)	4.53	4.63				4.59	4.64	5.47
fcc(110)	4.95	5.25				4.48	4.52	5.37
			ϕ (eV) computed by Methfessel, Hennig, and Scheffler[d]					
fcc(111)	4.98						4.67	
fcc(100)	4.49						4.43	
fcc(110)	4.19						4.23	
			ϕ (eV) computed by Skriver and Rosengaard[e]					
fcc(111)	5.09	5.09	2.10	2.23	4.63	5.3	5.01	6.01
fcc(100)			2.03	2.28		5.26	5.02	6.16
fcc(110)	5.34	5.62	2.09			4.48	4.40	5.40

[a]Reference 14.
[b]Reference 15.
[c]Reference 4.
[d]Reference 2.
[e]Reference 3.

III. THE EFFECT OF ADSORBED MONOLAYERS

It is well known that adsorption of a different atomic species on a substrate of a metal at the monolayer level can substantially affect the work function of the substrate—electropositive adsorbates lower the work function and electronegative adsorbates increase it. One of the most studied cases is that of Cs on W because of its technological importance for thermionic energy conversion. The classical work on this topic[16] showed that the work function of W decreases with the fraction of the substrate surface covered until a minimum work function of 1.68 eV is reached at a coverage of 0.67, after which it increases slowly, reaching that of pure Cs at a coverage of about three monolayers. More recent results[17] indicate that a minimum work function of 1.55 eV is attained. The difference between these results illustrates the experimental difficulties of measuring work functions to an accuracy of better than 0.1 eV.

TABLE II. Effective masses as a function of direction of motion within the crystal estimated from the measured work function for tungsten.

Direction	ϕ (eV) (measured)[a]	ε_F (eV)	m^*/m
[111]	4.47	10.46	0.87
[113]	4.18	10.46	0.795
[100]	4.63	10.46	0.91
[110]	5.25	10.46	1.09

[a]Reference 4.

The last atomic layer of the substrate and the partial atomic layer of the adsorbate form a complex system in which the Cs valence electrons in higher states transfer to lower unoccupied levels in the metal, thereby changing the electronic structure of the conduction band near the surface.[18] Equation (10) indicates that the work function decreases with increasing d (corresponding to decreasing ε_F [Eq. (17)]) and decreasing R. Since Cs has a much larger radius and a much smaller Fermi energy with W, it seemed reasonable to try to adapt the theory outlined in Sec. II, by assuming that the optimum substrate-adsorbate system has the Fermi energy of Cs and the radius of W. Using the LDA value for ε_F for Cs in Eq. (19) and R for W from Table I yields $\phi = 1.61$ eV for the monolayer, in remarkable agreement with the measured optimum value.

This result indicates why the minimum work function occurs at less than full coverage since a large fraction of the W substrate atoms must be exposed to the vacuum

TABLE III. Minimum work functions for adsorbed monolayers on refractory metals.

System	Calculated work function (eV)	Experiment[a]
W-Cs	1.61	1.55
W-Ba	2.20	2.5
Mo-Cs	1.60	1.65
Mo-Ba	2.19	2.9

[a]Reference 17.

for them to emit effectively. On the other hand, it seemed improbable, on initial consideration, that a fraction of a monolayer would be sufficient to develop a substrate-adsorbate system with a Fermi energy close to that of the bulk adsorbate material. For this reason Table III was constructed to compare the results using this approach and the data available from Table I, to the experimental results for W-Cs, W-Ba, Mo-Cs, and Mo-Ba.[17] The relatively close agreement between the experimental and calculated results indicates that the Fermi energies of the optimum monolayer cannot be far removed from that of the bulk adsorbate, and the procedure outlined above can be used with a degree of confidence to estimate work functions of adsorbed monolayer systems.

IV. VARIATION OF THE WORK FUNCTION OVER A LATTICE UNIT

The model for the surface of a crystal suggested by scanning tunneling microscopy (STM),[8] and reinforced by the fact that the work functions predicted using the atomic radius (and the accurate LDA values for the Fermi energy) are close to the measured work functions, is that of a plane with a regular array of hemispherical bumps of radius given by the atomic radius of the element concerned spaced on centers given by the lattice constants of the crystal face that it forms, as shown in Fig. 2. This surface is assumed to behave as a classical conductor to subatomic tolerances, for the purpose of calculating surface electric fields and the image force on a charge external to it.

The image force on an electron moving along a radial line joining the center of a hemisphere with its tip will initially, while it is close to the tip, be dominated by the spherical component. On the other hand, an electron leaving the flat part of the surface will be influenced by the planar image force over its entire journey, the influence of the surrounding hemispheres being both small and tending to cancel out. Thus, for constant d over the lattice site, the zero-field work function for an electron leaving the tip of a hemisphere will be close to that of an isolated sphere and lower than that for the plane part of the surface. The work function will increase to a value closer to the plane value as the departure point of an electron on the spherical surface moves away from the tip. In principle, the variation of the work function over the entire lattice site could be computed. The largest total change is given by Eq. (11) as

$$\delta\phi = 3.595/(2R+d) \text{ eV} .$$

Using the LDA values for Mo, W, and Ti from Table I, a total change in the work function from tip to plane of close to 1 eV is obtained. This work-function change would reduce the zero-field thermionic emission at 2500 K at the plane compared to that at the tip by about two orders of magnitude. Thus the effective emitting area must be substantially (perhaps 20–50 %) smaller than the total area. This casts doubt on the conventional practice of attributing the entire deviation of the measured Richardson A value[9] from the theoretical value to a temperature variation of the work function.[17] For Fowler-Nordheim field emission[19] and Schottky emission[9] the variation of the work function over a lattice site must be folded in with the variation of electric field over a lattice site to obtain a complete picture. This problem is considered in Sec. V.

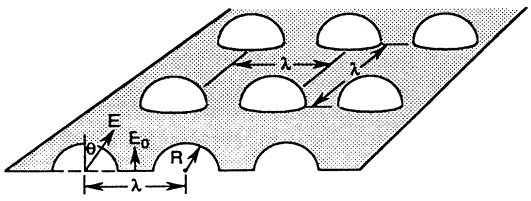

FIG. 2. Proposed model for the surface of an elemental metal crystal.

V. ELECTRIC FIELD DISTRIBUTION OVER A CONDUCTING SURFACE DEFINED BY AN ARRAY OF HEMISPHERES

To estimate the electric field variation over the surface, we first consider the well-known case[13] of a hemispherical bump on a plane electrode with a distant coplanar electrode. When a potential difference is applied, a uniform electric field E_0 exists perpendicular to the surface except in the vicinity of the bump where the solution to Laplace's equation with the appropriate boundary conditions gives the surface radial field as

$$E_r = 3E_0\cos\theta , \tag{20}$$

where θ is the angle between the normal through the center of the hemisphere and the radius vector.

The case of an array of hemispheres as shown in Fig. 2 does not have an analytic solution, and readily available computer programs for solving Laplace's equation do not allow for nonsimple, three-dimensional boundary conditions. However, since the lattice spacings are larger than those of the atomic diameters, the influence of the surrounding atoms is minimal for θ in a range of 0–30°. This has been verified using the program EGUN[20] with which we were able to solve the case of a hemisphere surrounded by a doughnut of the same radius. The shielding of the hemispherical surface by the doughnut will actually be greater than that of an array of hemispheres. The computer program was checked by first computing the hemispherical bump on a plane and then with the surrounding doughnut. The results for the worst case, where the doughnut is touching the hemisphere around a diameter (lattice spacing equal to atomic diameter), are

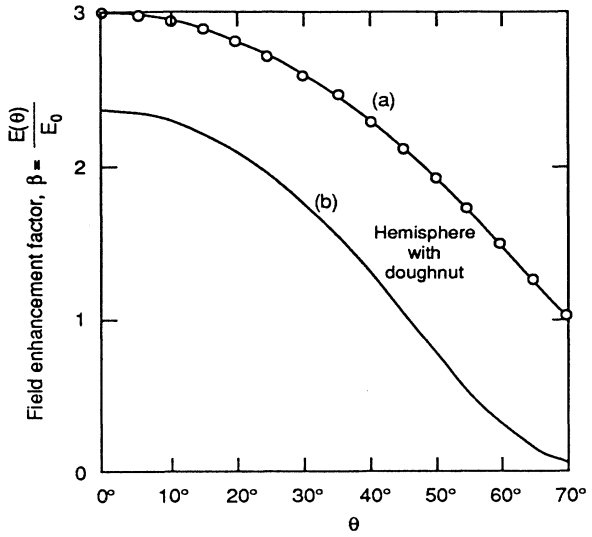

FIG. 3. Computed variation of normal surface electric field with polar angle for (a) a hemispherical bump on an infinite plane and (b) a hemispherical bump surrounded by a half doughnut of the same radius. E_0 is the background electric field calculated on the assumption that the electrode surface is perfectly smooth and of curvature very much larger than the hemisphere radius. $E(\theta)$ is the electric field at the surface of the hemisphere at angle θ to the normal. β is the field enhancement factor. Data denoted by open circles represent analytical value.

shown in Fig. 3. It will be seen that even in this case the field at the tip of the bump is only reduced from $3E_0$ for the single hemisphere to $2.37E_0$ for the hemisphere surrounded by a doughnut. The cosine variation with θ remains valid up to about 25° after which the variation is faster. At 30° the field at the tip of the single hemisphere is $2.6E_0$ (a 13% drop) compared with $1.76E_0$ (a 26% drop) for the doughnut case.

For Fowler-Nordheim emission[19] using $\phi=4.4$ eV (Mo), a change of E from 6×10^9 V m^{-1} to 5×10^9 V m^{-1} (a 17% change) results in a reduction in current density by nearly two orders of magnitude.

For Schottky emission, the lowering of the work function for a plane surface is given by Eq. (5) as

$$\Delta\phi=3.79\times10^{-5}E^{1/2}\ \text{eV}$$

for E in V m^{-1} so that at the tip of the hemisphere it is

$$\Delta\phi\sim5.99\times10^{-5}E_0^{1/2}\ \text{eV}\ . \tag{21}$$

The difference between the field-induced change in work function at the hemisphere tip and the plane part of the lattice unit is always a factor of $\sim(2.5)^{1/2}=1.58$. Thus, if the reduction of the work function is 0.5 eV at the tip ($E_0\sim7\times10^7$ V m^{-1}), the reduction at the planar part of the surface will be 0.32 eV. However, at 2500 K a difference in work function of $(0.5-0.32)=0.18$ eV causes the current density to change by a factor of 2.3. Thus the integrated thermionic emission due to the Schottky lowering of the work function for an array of hemispheres will be somewhat greater than that predicted for the case of a plane cathode [Eq. (5)] for the same applied voltage.

Taking into account the inexactness of the model we may use as a first approximation for estimating the emission under the action of an electric field

$$\begin{aligned} &E_r\sim2.5E_0\ ,\quad 0<\theta<20°\ ,\\ &E_r\sim E_0\ ,\quad \theta>20°\ . \end{aligned} \tag{22}$$

Thus the high emitting area over a lattice site will be $\sim\pi R^2\tan^2 20°$. The ratio of the high emitting area to the total area will then be approximately $0.42R^2/\lambda_1\lambda_2$ (where λ_1 and λ_2 are lengths of the sides of the rectangular lattice), which usually has a value in a range of 0.1–0.2. Thus the effect for Schottky emission will be to increase the total current per lattice site, in the example given above, by approximately 20–50 %. But in the case of Fowler-Nordheim emission, effectively only the high emitting area is contributing to the total emission, giving the average emission density over a lattice site about 10–20 % of that at the tip (but still substantially greater than that of a perfectly planar surface).

VI. VARIATION OF THE WORK FUNCTION WITH STRAIN

Less exact values of the Fermi energy can be obtained from the simple zero-order approximation (ZOA) for the electron gas inside a metal that was originally used to obtain the Richardson-Dushman equation for thermionic emission of electrons with zero field at the emitting surface.[9] The ZOA gives the Fermi energy as

$$\begin{aligned} \varepsilon_F&=(h^2/2m^*)(3N/8\pi)^{2/3}\\ &=5.842\times10^{-38}\times m/m^*\times N^{2/3}\ \text{J}\ , \end{aligned} \tag{23}$$

where N is the number of electrons per unit volume—that is,

$$\varepsilon_F=3.651\times10^{-19}\times m/m^*\times N^{2/3}\ \text{eV}\ . \tag{24}$$

Combining Eqs. (18) with Eq. (24) and assuming $m/m^*\sim1$ gives

$$\begin{aligned} \phi&=1.23\times10^{-9}N^{1/3}[1+1.62\times10^9/RN^{1/3}]^{-1}\\ &=AN^{1/3}[1+BN^{-1/3}]^{-1}\ , \end{aligned} \tag{25}$$

where

$$A=1.236\times10^{-9}\ \text{ and }\ B=1.617\times10^9/R\ . \tag{26}$$

Now N = (number of conduction electrons per atom n)$\times$ (density ρ)/[(molecular weight M)$\times$ (weight of an amu)], that is

$$N=n\rho/(M\times1.66\times10^{-27})\ \text{electrons/m}^3\ . \tag{27}$$

Fermi energies calculated using the ZOA, using Eq. (27) in (24) and $m/m^*=1$, usually differ from those calculated using the LDA by at most a few eV (for example, ZOA values for Mo and W are 5.77 and 9.19 eV, respectively, compared with LDA values of 8.01 and 10.46), giving corresponding differences in the values predicted

for the work function using the method described in Sec. II. However, the results are close enough to argue that the ZOA may be used to predict approximately the variation of the work function with strain caused by a rise in temperature or applied stress.

It is well known that the work function of many materials is temperature dependent[17] with average coefficient α in a range of 10^{-5}–10^{-3} eV/K. This can be associated with the expansion of the material with increasing temperature, as follows.

From Eq. (25) we have

$$d\phi/dN=[A/3N][(N^{1/3}+2AB)(1+BN^{-1/3})^{-2}] . \quad (28)$$

Now

$$\frac{d\phi}{dT}=\frac{d\phi}{dN}\frac{dN}{dT} \quad (29)$$

and

$$N=n/V , \quad (30)$$

where n is the number of electrons per unit cell and V is the volume of a unit cell,

$$V(T)\sim V(0)(1+3\gamma T) , \quad (31)$$

where $V(T)$ is the volume of a unit cell at T K and γ is the coefficient of linear expansion. Thus

$$N(T)=N(0)(1+3\gamma T)^{-1}\sim N(0)(1-3\gamma T) \quad \text{(since } 3\gamma T\ll 1\text{)} \quad (32)$$

and hence

$$dN/dT\sim -N(0)3\gamma , \quad (33)$$

giving

$$d\phi/dT\sim -[\gamma A][(N^{1/3}+2AB)(1+BN^{-1/3})^{-2}] . \quad (34)$$

For W, $R=1.41$ Å, $\gamma\sim 5.3\times 10^{-6}$/K (at 1400 K), and using $\rho=19.3\times 10^{3}$ kg/m^3, $n=2$ electrons/atom, and $M=184$ amu we obtain $N=1.26\times 10^{29}$ electrons/m^3. Thus from Eq. (33) we obtain

$$d\phi/dT\sim -2.16\times 10^{-5} \text{ eV/K} \quad (35)$$

in order-of-magnitude agreement with the experimental values for the (112) and (100) faces of W in a range of 1700–2000 K, which are -8.3×10^{-5} and -1.7×10^{-5} eV/K, respectively.[17]

This order-of-magnitude agreement given by combining Eq. (19) for the work function by using the ZOA for the Fermi energy is striking and implies that change in N with increasing T is a factor. However, the fact that some crystal faces have positive coefficients indicates, as expected, that the ZOA is not taking into account all the factors involved. Other factors have been discussed by Herring and Nichol.[21]

Note that γ increases with increasing temperature and at 2000 K reaches a value of 6.4×10^{-6} for W. Since needle-shaped field-emission cathodes heat up with increasing current to the point where they can disrupt by melting,[22] the work function could change by over 0.1 eV at the high current densities obtained near breakdown. This effect could contribute to the deviations from the Fowler-Nordheim relation observed at high currents. Smaller than expected currents are usually attributed to space charge.[23]

The above discussion indicates that any change in the size of the lattice unit cell will give rise to a change in the work function. The tensile stress induced on the cathode surface by an electric field may be considered approximately isostatic and is given by

$$F=\xi_0 E^2/2=4.42\times 10^{-12}E^2 \text{ N/m}^2=CE^2 . \quad (36)$$

The change in volume due to a uniform tensile stress F is given by

$$V(F)=V(0)(1+F/M) , \quad (37)$$

where M is the bulk modulus. Hence

$$N(F)=N(0)/(1+F/M) =N(0)/(1+CE^2/M)\sim N(0)(1-CE^2/M) \quad (38)$$

since $CE^2/M\ll 1$.

Using Eqs. (25) and (36)

$$\phi(E)=AN(0)^{1/3}(1-CE^2/M)^{1/3} \times\{1+B/R[N(0)(1-CE^2/M)]^{1/3}\}^{-1} \quad (39)$$

$$\sim AN(0)^{1/3}[1+B/RN(0)^{1/3}]^{-1}(1-CE^2/3M) \sim\phi(0)(1-CE^2/3M) . \quad (40)$$

Hence

$$\Delta\phi=\phi(0)-\phi(E)=-\phi(0)CE^2/3M . \quad (41)$$

For W, we use $\phi(0)=4.55$ eV and $M=3.2\times 10^{11}$ N/m^2.[24] With E in the field-emission range (say, 7×10^{9} V/m), this gives

$$\Delta\phi\sim -1.03\times 10^{-3} \text{ eV}. \quad (42)$$

This value is too small to have any substantial effect on the field-emission current density. Note that the bulk modulus changes less with stress until the yield point is reached; however, the bulk modulus does decrease with increasing temperature, and the associated work-function change could become comparable with that due to thermal expansion at temperatures approaching the melting point.

VII. DISCUSSION

A simple procedure has been found that is able to predict the work function of metals, and the optimum work functions for monolayers of electropositive elements on metal substrates, within a few tenths of an eV, as well as or better than the more comprehensive methods.[2,3] The procedure works well for metals from disparate parts of the periodic table. The physical significance of this result is that the Heisenberg uncertainty distance can be identified with the distance at which the image force on an electron external to the surface begins to act *and* the

surface structure on an atomic scale must be taken into account.

The postulate of a distance from the surface at which the classical image force begins to act was at the core of the early theories of field-electron-emission phenomena (Schottky and Fowler-Nordheim emission).[9,19] The remarkable agreement between the simple approach presented here and experiment justifies the concept of continuous decoherence[5–7] in which it is proposed that "the environment surrounding a quantum system can, in effect, monitor some of the system's observables. As a result, the eigenstates of those observables continuously decohere and can behave as classical states."[7] In the present model, two surfaces are identified. The first surface behaves as a defining boundary for electrons inside the metal and as a classical metal surface for electrons on the vacuum side some distance from it. The second surface is that at which an electron approaching from the interior will have lost all its momentum in the escape direction. Between these two surfaces is a region in which the state of the electron continuously decoheres from quantum states at the first boundary to classical states at the second. The distance between the two surfaces is given in this case by the position uncertainty of the electron, which, for an electron with the Fermi energy, is about half the atomic radius.

The work function of the various crystal faces of the same material could be estimated by this method if values of the effective mass of the escaping electron with orientation within the crystal were known but this is difficult to find out both theoretically and experimentally. Alternatively, if the validity of the present approach is accepted then the LDA values of the Fermi energy combined with an experimental value for the work function for specific crystal faces enables an estimate of the effective mass to be made and appears to give reasonable values.

Computed values for the variation of electric field (generated by a distant external electrode at a positive potential with respect to the cathode) over a cathode surface with topographical structure on an atomic scale were obtained by solving Laplace's equation. The results indicate that the field at the tips of the surface atoms is approximately 2.5 times that estimated on the basis that the surface is perfectly smooth. Initially, the surface field decreases gradually with distance from the tip and then much more rapidly until it approaches the "smooth flat" value. This effect means that most emitted electrons come from the tips of the atoms, reducing the effective emission area compared with the total surface area. This effect is of marginal significance for thermionic emission in the low-field, Schottky region, but of major importance for the high-field, low-temperature, Fowler-Nordheim region because the image force is dominated by the atomic radius and not the macroscopic curvature of the cathode surface.

For vacuum microelectronic devices, very small field-emission electron sources are often used.[25] These consist of metal cones about 1 μm high with a tip radius of curvature of about 200 Å. The accelerating electrode has a hole coaxial with the cone of radius of about 0.5 μm to allow the electrons to be injected into the operational region. A number of computations using different programs have been used to estimate the electric field around the tip.[26,27] All have produced field values about 2.5 times smaller than that required to explain the experimental results on the basis of the Fowler-Nordheim equation. Previous attempts to explain this effect have been to assume that the emission comes from an increased field due to isolated individual atoms resting on a surface,[26] a low-work-function atom embedded in the surface,[27] or the change in image force due to the macroscopic radius at the apex of the cone.[28]

The results of the research reported in this paper suggest that the factor of 2.5 is due to the microscopic curvature of the tips of the atoms themselves magnifying a macroscopic background field. Once sufficiently removed for the image force to be dominated by the macroscopic curvature, the electron is too far away for this to substantially affect the work function. Note that the electric field at the tip of a single atom resting on a surface comprising an array of atoms is larger but will not be much larger than that at the tips of the atoms of the array itself, but may be sufficient for this atom to dominate the field emission from the surface due to the exponential dependence of the emission on the electric field.

Before the advent of modern high-speed computers, attempts were made to estimate the field at the tip of conventional freestanding single crystals typically a few thousand angstroms in radius, based on the assumption that the Fowler-Nordheim equation was valid[19] and $E=\beta V$ over a constant emitting area. In this case, adjustment of the β factor would automatically take into account the field enhancement due to the atomic surface structure, in addition to the macroscopic tip radius.

Since the ZOA enables order-of-magnitude estimates to be made of work functions it may be expected to give order-of-magnitude estimates of the change in work function with strain. The predicted decrease in work function with temperature due to thermal expansion using the ZOA is in fact shown to be of the same order as those observed, but the theory does not account for the observation that some crystal faces show an increase in work function with increasing temperature. Any decrease in work function with field-induced tensile stress does not appear to be important even at the very high fields required for Fowler-Nordheim emission, unless the temperature becomes high enough to substantially decrease the bulk modulus.

ACKNOWLEDGMENTS

The author expresses his gratitude to ARPA (under Contract No. MDA972-91-C-0029) and SRI International for supporting this work. Invaluable discussions were held with Arden Sher, Mark van Schilfgaarde, Paul Schwoebel, and Arne Rosengreen (now deceased) of SRI's Physical Electronics Laboratory, Professor Paul Cutler of Pennsylvania State University, and Jules Levine of Texas Instruments.

*FAX: (415) 859-3090.
[1]A. Sher, M. van Schilfgaarde, and M. A. Berding, J. Vac. Sci. Technol. B **9**, 1738 (1991).
[2]M. Methfessel, D. Hennig, and M. M. Scheffler, Phys. Rev. B **46**, 4816 (1992).
[3]H. L. Skriver and N. M. Rosengaard, Phys. Rev. B **46**, 7157 (1992).
[4]H. B. Michaelson, J. Appl. Phys. **48**, 7729 (1977).
[5]H. Everett III, Rev. Mod. Phys. **29**, 454 (1957).
[6]*The Many Worlds Interpretation of Quantum Mechanics,* edited by B. S. DeWitt and N. Graham (Princeton University Press, Princeton, NJ, 1973).
[7]W. H. Zurek, Phys. Today **44**(10), 36 (1991).
[8]C. J. Chen, *Introduction to Scanning Tunneling Microscopy* (Oxford University Press, Oxford, 1993).
[9]W. B. Nottingham, in *Thermionic Emission,* edited by S. Flugge, Electron Emission-Gas Discharges I Vol. 21 (Springer-Verlag, Berlin, 1956), pp. 1–174.
[10]A. G. Aguiluz and W. Hanke, Phys. Rev. B **39**, 10 433 (1989).
[11]A. G Aguiluz, M. Heinrichsmeir, and W. Hanke, Phys. Rev. Lett. **68**, 1359 (1992).
[12]R. P. Feynman, R. B. Leighton, and M. Sands, *The Feynman Lectures on Physics* (Addison-Wesley, Reading, MA, 1965), Vol. III, pp. 2–6.
[13]C. Maxwell, *Electricity and Magnetism* (Dover, New York, 1891).
[14]*American Institute of Physics Handbook,* 3rd ed. (McGraw-Hill, New York, 1972).
[15]A. Paxton and M. van Schilfgaarde (private communication).
[16]J. B. Taylor and I. Langmuir, Phys. Rev. **44**, 423 (1933).
[17]G. A. Haas, in *Methods of Experimental Physics,* edited by L. Marton (Academic, New York, 1967), Vol. 4, pp. 1–38.
[18]K. F. Wojciechowski, in *Progress in Surface Science,* edited by G. Davison (Pergamon, Oxford, 1971), Vol. 1, Pt. 1, pp. 65–104.
[19]R. H. Good and E. W. Müller, in *Field Emission,* edited by S. Flugge, Handbüch der Physik Electron Emission-Gas Discharges I Vol. 21 (Springer-Verlag, Berlin, 1956), pp. 176–231.
[20]W. B. Herrmannsfeldt (unpublished).
[21]C. Herring and M. H. Nichol, Rev. Mod. Phys. **21**, 185 (1949).
[22]I. Brodie, Int. J. Electron. **18**, 223 (1965).
[23]W. P. Dyke and W. W. Dolan, in *Advances in Electronics and Electron Physics,* edited by L. Marton (Academic, New York, 1956), Vol. 8, pp. 90–185.
[24]C. Kittel, *Introduction to Solid State Physics* (Wiley, New York, 1986), p. 57.
[25]I. Brodie and C. A. Spindt, Adv. Electron. Electron Phys. **83**, 1 (1992).
[26]C. A. Spindt, I. Brodie, I. Humphrey, and E. R. Westerberg, J. Appl. Phys. **47**, 5248 (1976).
[27]W. B. Herrmannsfeldt, R. Becker, I. Brodie, A. Rosengreen, and C. A. Spindt, Nucl. Instrum. Methods A **298**, 39 (1990).
[28]J. He, P. H. Cutler, and N. M. Miscovsky, Appl. Phys. Lett. **59**, 1644 (1991).